Supporting Information

When Does the IC_{50} Accurately Assess the Blocking Potency of a Drug?

Julio Gomis-Tena, Brandon M. Brown, Jordi Cano, Beatriz Trenor, Pei-Chi Yang, Javier Saiz, Colleen E. Clancy, Lucia Romero[*].

[a]Centro de Investigación e Innovación en Bioingeniería (Ci2B), Universitat Politècnica de València, Camino de Vera, s/n, 46022, Valencia, Spain.

[b]Department of Pharmacology, One Shields Avenue, University of California, Davis, Davis, CA 95616-8636, United States.

*Corresponding Author e-mail: lurope@ci2b.upv.es

Table S1. Kinetic rates of the simulated drug-I_{Kr} interactions. Corresponding Markovian models (first column) are shown in *Figure 1 of the main article*, and k and r are the diffusion and the dissociation rates, respectively.

Configuration	Name	Closed		Open		Inactivated	
		k$(\mu M^{-1}s^{-1})$	**r**(s^{-1})	**k**$(\mu M^{-1}s^{-1})$	**r**(s^{-1})	**k**$(\mu M^{-1}s^{-1})$	**r**(s^{-1})
A and B	Closed_s	1	0.01				
	Closed_m	1	0.1				
	Closed_f	1	1				
	Closed_ff	10	10				
C and D	Open_s			1	0.01		
	Open_m			1	0.1		
	Open_f			1	1		
	Open_ff			10	10		
E and F	Inactivated_s					1	0.01
	Inactivated_m					1	0.1
	Inactivated_f					1	1
	Inactivated_ff					10	10
G and H	ClosedO_sss	1	0.001	1	0.1		
	ClosedO_ss	1	0.003	1	0.3		
	ClosedO_s	1	0.01	1	1		
	ClosedO_m	1	0.1	1	10		
	ClosedO_f	1	1	1	100		
	ClosedO_ff	10	10	10	1000		
	OpenC_sss	1	0.1	1	0.001		
	OpenC_ss	1	0.3	1	0.003		
	OpenC_s	1	1	1	0.01		
	OpenC_m	1	10	1	0.1		
	OpenC_f	1	100	1	1		
	OpenC_ff	10	1000	10	10		
	CO_sss	1	0.001	1	0.001		
	CO_ss	1	0.003	1	0.003		
	CO_s	1	0.01	1	0.01		
	CO_m	1	0.1	1	0.1		
	CO_f	1	1	1	1		
	CO_ff	10	10	10	10		
I and J	OpenI_sss			1	0.001	1	0.1
	OpenI_ss			1	0.003	1	0.3
	OpenI_s			1	0.01	1	1
	OpenI_m			1	0.1	1	10
	OpenI_f			1	1	1	100
	OpenI_ff			10	10	10	1000
	InactivO_sss			1	0.1	1	0.001
	InactivO_ss			1	0.3	1	0.003
	InactivO_s			1	1	1	0.01
	InactivO_m			1	10	1	0.1
	InactivO_f			1	100	1	1
	InactivO_ff			10	1000	10	10

Table S2. Kinetic rates of the simulated drug-I_{Kr} interactions. Corresponding Markovian models (first column) are shown in *Figure 1 of the main article*, and k and r are the diffusion and the dissociation rates, respectively.

Configuration	Name	Closed		Open		Inactivated	
		k$(\mu M^{-1}s^{-1})$	**r**(s^{-1})	**k**$(\mu M^{-1}s^{-1})$	**r**(s^{-1})	**k**$(\mu M^{-1}s^{-1})$	**r**(s^{-1})
I and J	IO_sss			1	0.001	1	0.001
	IO_ss			1	0.003	1	0.003
	IO_s			1	0.01	1	0.01
	IO_m			1	0.1	1	0.1
	IO_f			1	1	1	1
	IO_ff			10	10	10	10
K and L	ClosedOI_sss	1	0.001	1	0.1	1	0.1
	ClosedOI_ss	1	0.003	1	0.3	1	0.3
	ClosedOI_s	1	0.01	1	1	1	1
	ClosedOI_m	1	0.1	1	10	1	10
	ClosedOI_f	1	1	1	100	1	100
	ClosedOI_ff	10	10	10	1000	10	1000
	OpenCI_sss	1	0.1	1	0.001	1	0.1
	OpenCI_ss	1	0.3	1	0.003	1	0.3
	OpenCI_s	1	1	1	0.01	1	1
	OpenCI_m	1	10	1	0.1	1	10
	OpenCI_f	1	100	1	1	1	100
	OpenCI_ff	10	1000	10	10	10	1000
	InactivOC_sss	1	0.1	1	0.1	1	0.001
	InactivOC_ss	1	0.3	1	0.3	1	0.003
	InactivOC_s	1	1	1	1	1	0.01
	InactivOC_m	1	10	1	10	1	0.1
	InactivOC_f	1	100	1	100	1	1
	InactivOC_ff	10	1000	10	1000	10	10
	COI_sss	1	0.001	1	0.001	1	0.001
	COI_ss	1	0.003	1	0.003	1	0.003
	COI_s	1	0.01	1	0.01	1	0.01
	COI_m	1	0.1	1	0.1	1	0.1
	COI_f	1	1	1	1	1	1
	COI_ff	10	10	10	10	10	10

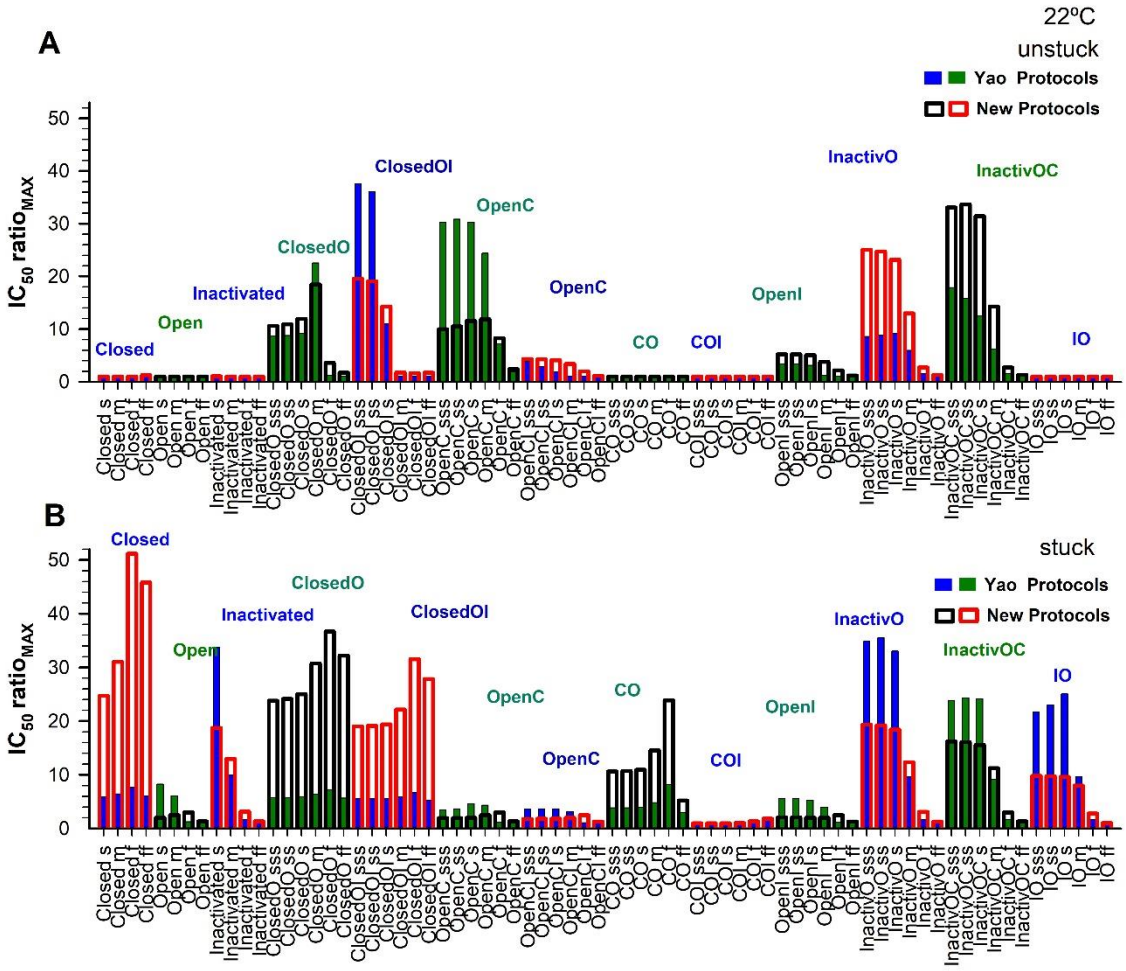

Figure S1. Maximum IC_{50} ratios for unstuck (top panel) and stuck (bottom panel) drugs obtained with our protocols (non-filled bars) and with Yao, et al. 2005[1] protocols (filled bars) at 22ºC.

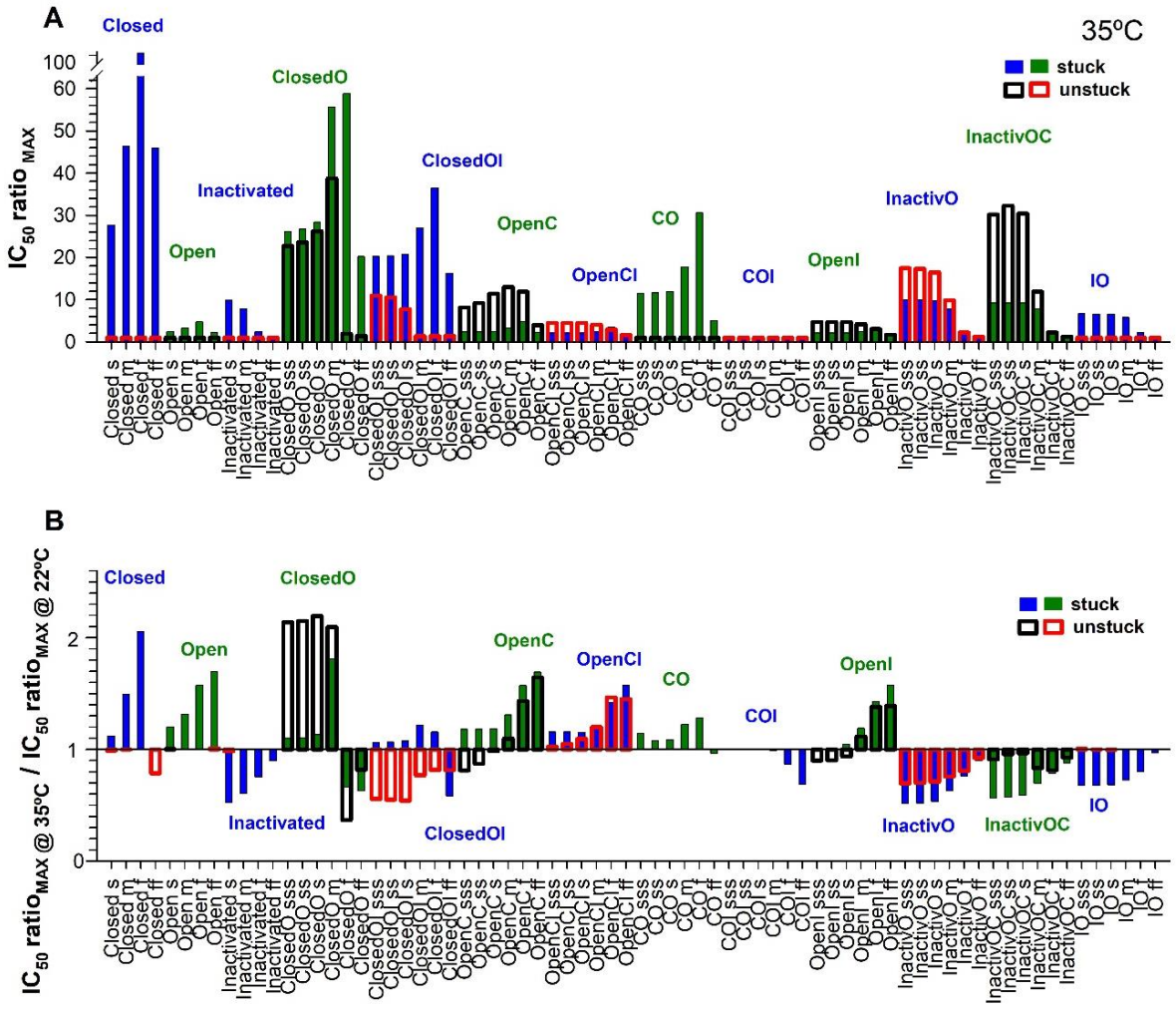

Figure S2. Maximum IC_{50} ratios obtained with our proposed protocols (P0, P40 and P-80) at 35ºC (A) and comparison with 22ºC (B). A: IC_{50} ratios for each prototypical drug at 35ºC. Filled (green and blue) and non-filled (black and red) bars for stuck and unstuck drugs, respectively. B: maximum IC_{50} ratios at 35ºC relative to those observed at 22ºC. In order to compare previous results directly to those obtained at 22ºC, the maximum IC_{50} ratio at 35ºC was normalized to the maximum IC_{50} ratio at 22ºC (ratio_35_22). Colored bars in Panel B are depicted from unity to the value of ratio_35_22. Stuck and unstuck refer to the state of the channel when the drug is bound.

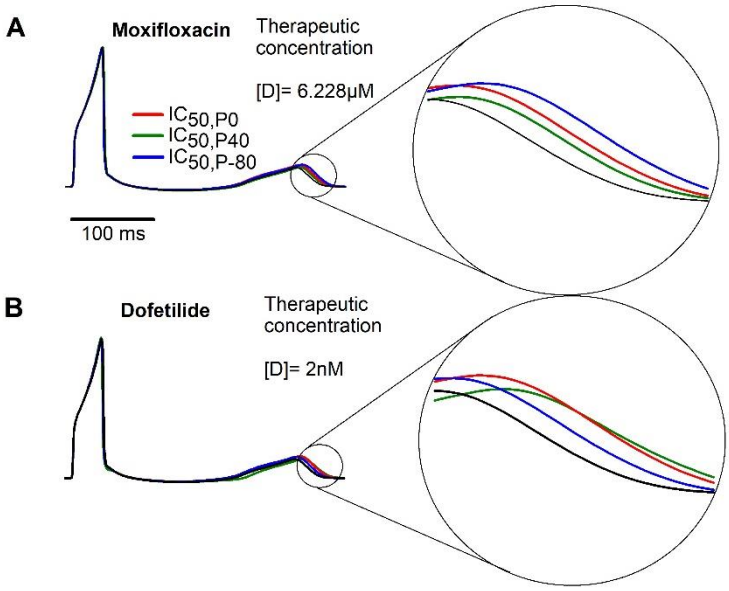

Figure S3. Simulated steady state pseudo-ECGs for moxifloxacin (top row) and dofetilide (bottom row). Simulated steady state pseudo-ECG in control (black) and in the presence of 6.228 μM of moxifloxacin and 2 nM of dofetilide considering the IC_{50} obtained using the P-80 (blue), P0 (red) and P40 (green).

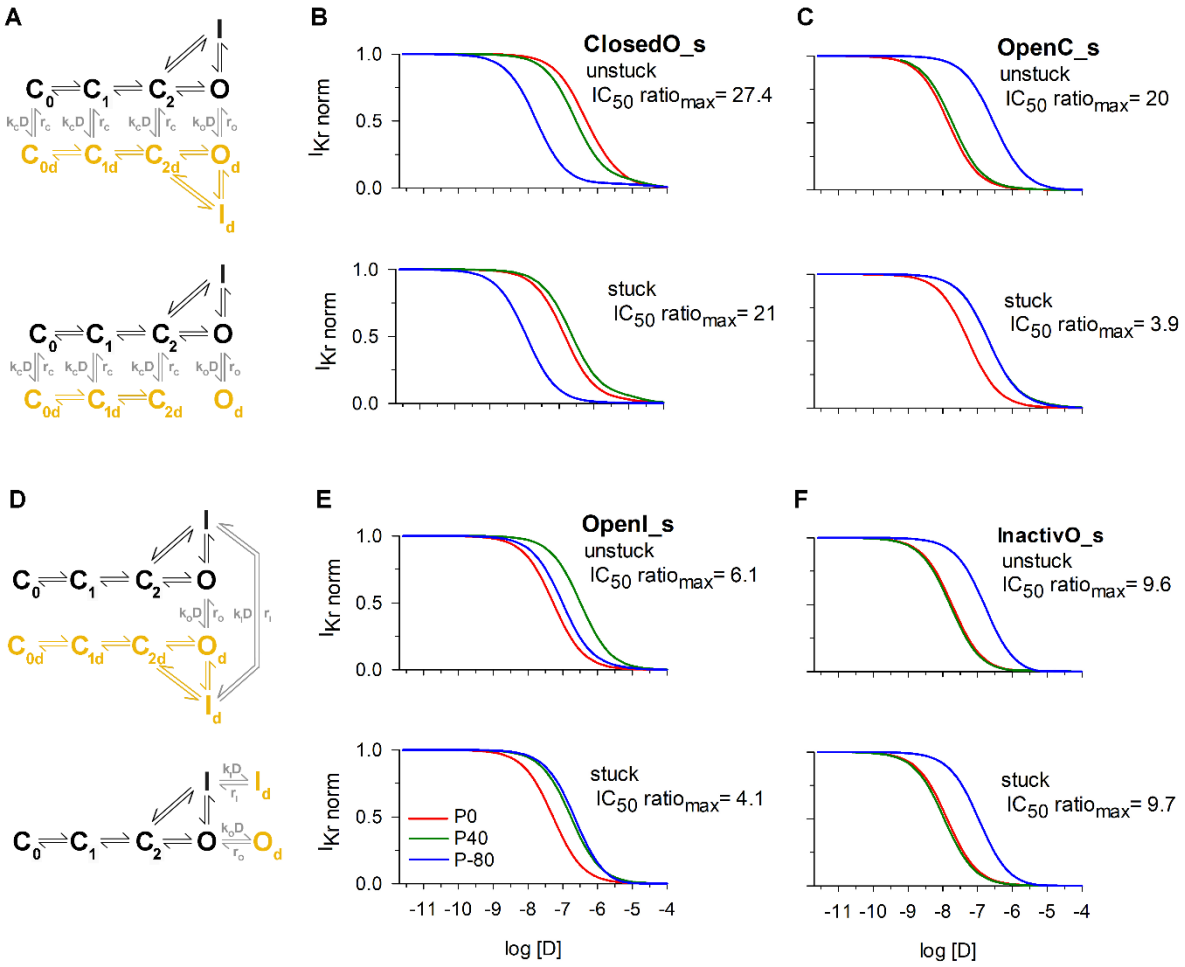

Figure S4. Simulated Hill plots for each type of the prototypical drugs binding to two states with state-dependent affinities using the proposed protocols: P-80 (blue), P0 (red) and P40 (green) at 22ºC using Lee et al. hERG model[2]. Left column shows the Markovian schemes of the drug-channel interactions of each row (A and D): unstuck (top) and stuck (bottom) variants of ClosedO_s (B), OpenC_s (C), OpenI_s (E) and InactivO_s (F). Unbound states are depicted in black and transitions between them are defined as in[2], drug-bound states are depicted in yellow and transition between unbound and drug-bound channels are depicted in gray. Microscopic reversibility was ensured by equaling the product of the rates going clockwise to the product going anticlockwise in closed loops[3]. As drug-bound channels are electrically silent, which precludes the assessment of the transition rates between states, we modified the transition rates from I_d to O_d, from O_d to $C2_d$ and from I_d to $C2_d$ when appropriate. The maximum IC_{50} ratio for each drug is also indicated in each panel.

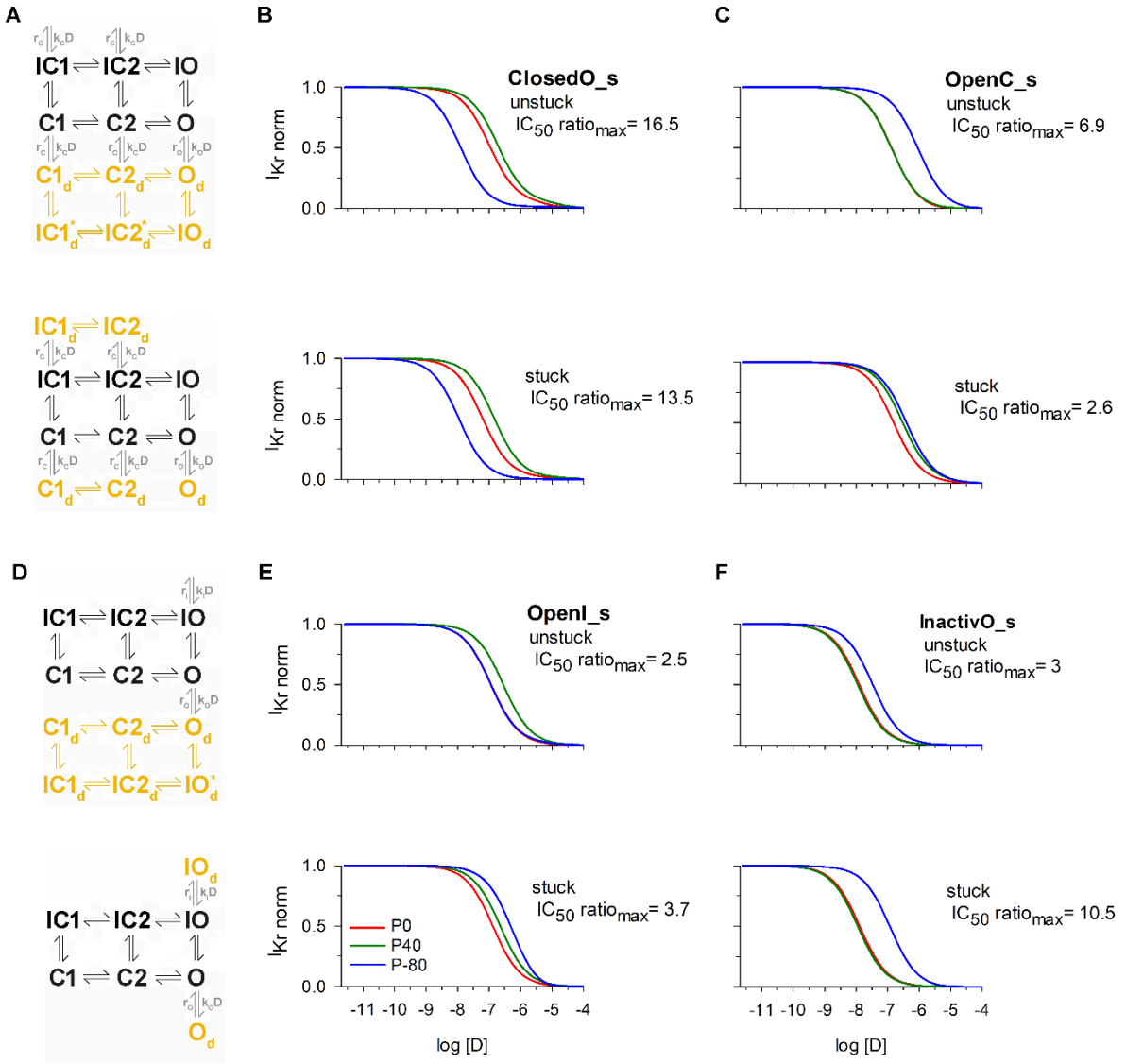

Figure S5. Simulated Hill plots for each type of the prototypical drugs binding to two states with state-dependent affinities using the proposed protocols: P-80 (blue), P0 (red) and P40 (green) at 22ºC using Li et al. hERG model[4]. Left column shows the Markovian schemes of the drug-channel interactions of each row: unstuck (top) and stuck (bottom) variants of ClosedO_s (B), OpenC_s (C), OpenI_s (E) and InactivO_s (F). Unbound states are depicted in black and transitions between them are defined as in[4], drug-bound states are depicted in yellow and transition between unbound and drug-bound channels are depicted in gray. Transition rates between IC1 and $IC1_d$, IC2 and $IC2_d$ and IO and IO_d are depicted at the top of IC1, IC2 and IO and the asterisks in IC1d, IC2d and IO_d indicate that they are connected to IC1, IC2 and IO, respectively, by means of these transition rates (top panels in A and D). Microscopic reversibility was ensured by equaling the product of the rates going clockwise to the product going anticlockwise in closed loops[3]. As drug-bound channels are electrically silent, which precludes the assessment of the transition rates between states, we modified the transition rates from I_d to O_d, from O_d to $C2_d$ and from I_d to $C2_d$ when appropriate. The maximum IC_{50} ratio for each drug is also indicated in each panel.

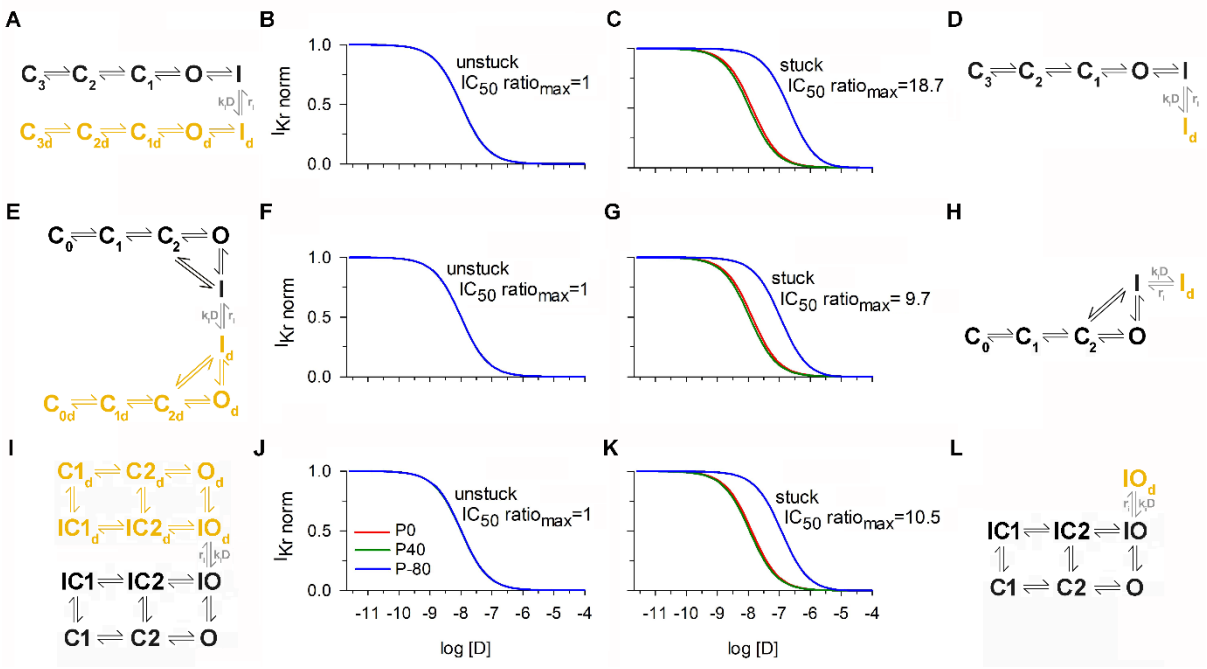

Figure S6. Simulated Hill plots for unstuck and stuck Inactivated_s using three ionic channel models: Fink et al[5] (B and C), Lee et al.[2] (F and G) and Li et al.[4] (J and K) models, and the corresponding Markovian schemes of the unstuck and stuck drug-channel interactions (A and D, E and H, and I and L, respectively). Unbound states are depicted in black, drug-bound states are depicted in yellow and transition between unbound and drug-bound channels are depicted in gray. The maximum IC_{50} ratio for each drug is also indicated in each panel.

References

(1) Yao, J.-A.; Du, X.; Lu, D.; Baker, R. L.; Daharsh, E.; Atterson, P. Estimation of Potency of HERG Channel Blockers: Impact of Voltage Protocol and Temperature. *J. Pharmacol. Toxicol. Methods* **2005**, *52*, 146–153. https://doi.org/10.1016/j.vascn.2005.04.008.

(2) Lee, W.; Mann, S. A.; Windley, M. J.; Imtiaz, M. S.; Vandenberg, J. I.; Hill, A. P. In-Silico Assessment of Kinetics and State Dependent Binding Properties of Drugs Causing Acquired LQTS. *Prog. Biophys. Mol. Biol.* **2016**, *120*, 89–99. https://doi.org/10.1016/j.pbiomolbio.2015.12.005.

(3) Colquhoun, D.; Dowsland, K. a; Beato, M.; Plested, A. J. R. How to Impose Microscopic Reversibility in Complex Reaction Mechanisms. *Biophys. J.* **2004**, *86*, 3510–3518. https://doi.org/10.1529/biophysj.103.038679.

(4) Li, Z.; Dutta, S.; Sheng, J.; Tran, P. N.; Wu, W.; Colatsky, T. A Temperature-Dependent in Silico Model of the Human Ether-à-Go-Go-Related (HERG) Gene Channel. *J. Pharmacol. Toxicol. Methods 81*, 233–239. https://doi.org/10.1016/j.vascn.2016.05.005.

(5) Fink, M.; Noble, D.; Virag, L.; Varro, A.; Giles, W. R. Contributions of HERG K+ Current to Repolarization of the Human Ventricular Action Potential. *Prog. Biophys. Mol. Biol.* **2008**, *96*, 357–376. https://doi.org/10.1016/j.pbiomolbio.2007.07.011.